

Scanning electron microscopy investigation of loess soil stabilized with cement and natural zeolite

Boriana Tchakalova, Tzvetoslav Iliev

Geological Institute Bulgarian Academy of Sciences, Acad. G. Bonchev Str., Bl. 24, 1113 Sofia, Bulgaria;
e-mails: boriana@geology.bas.bg, tz_iliev@abv.bg

(Received: 01 March 2022; accepted in revised form: 29 March 2022)

Abstract. Zeolite and Portland cement have been used to stabilize a loess soil from the region of Kozloduy (North Bulgaria). This paper examines the microstructural behavior of cement–zeolite treated loess soil without compaction at water content higher than optimum. Scanning electron microscopy and semi-quantitative energy dispersive spectroscopy analyses on stabilized loess were carried out after various curing periods. The identification of the formation of cementitious products in treated loess soil was conducted by SEM–EDS spectral analysis. Based on the study of the microstructural development, it was found that the modified loess microstructure undergoes significant modifications during the observed period.

Tchakalova, B., Iliev, T. 2022. Scanning electron microscopy investigation of loess soil stabilized with cement and natural zeolite. *Geologica Balcanica* 51 (1), 15–21.

Keywords: loess soil, cement-zeolite, non-compacted stabilization, soil microstructure.

INTRODUCTION

Specific geotechnical problems complicate construction in loess soil due to its strong sensitivity to water content increase and ground collapse consequentially. Soil stabilization is a method used to change properties of problematic soils to enhance their geotechnical behavior. Stabilization with or without compaction (plastic soil–cement) has been widely applied to improve loess ground. There are various cement based pozzolanic materials, and different additives, that can be used to improve engineering properties of loess soil.

Zeolites are a large group of natural aluminosilicates containing more than 50 natural and 150 synthetic zeolites. Because of their pozzolanic activity, they are often used in soil stabilization and the construction industry. Similar to other pozzolanic materials, zeolite addition can improve the strength of

stabilized soil by pozzolanic reaction with $\text{Ca}(\text{OH})_2$ (Poon *et al.*, 1999). In addition, due to the higher specific surface area available for reaction, the open zeolite structure is thought to contribute to increased reactivity. It has been reported that natural zeolites could be used for improving the strength, durability, impermeability and interfacial microstructure of mortars, concrete and soils (Türköz and Vural, 2013; Mola-Abasi *et al.*, 2016; Salamatpoor *et al.*, 2018).

Due to cement hydration reaction in stabilized soils, chemical processes and physical transformations take place (Evstatiev, 1984; Glasser *et al.*, 1986). The hydration process begins fast during the first month, and then gradually retards. At the early stages of hydration, the cement dissolves into the soil pore spaces and begins formation of new phases such as calcium–silicate hydrates (C–S–H), calcium–aluminum hydrates (C–A–H), and calcium–aluminum–

silicate hydrates (C–A–S–H). The improvement of the mechanical properties of the stabilized soil is a result of embodiment of these cementitious products in the soil matrix. It is known that the changes in engineering properties are directly related to the change in microstructure (Angelova and Evstatiev, 1990). Consequently, it is important to assign microstructural changes that occur in order to determine how the additives affect structure.

The interdependence between stabilized soil microstructure and strength development has been studied insufficiently because, generally, engineering tests have been applied to determine improvement effect. Scanning electron microscopy (SEM) has been effectively applied to study the stabilization effect (Angelova and Evstatiev, 1990; Nontananandh *et al.*, 2005; Kamruzzaman *et al.*, 2006; Antonov, 2013; Romero, 2013; Ural, 2021, Quadri *et al.*, 2022).

The literature analysis indicates that only limited information is available on the microstructure of plastic soil cement. The aim of the present paper is to investigate the microstructural peculiarities of cement–zeolite treated loess soil without compaction to derive a modified soil with less deformation and permeability characteristics.

MATERIALS AND METHODS

Loess soil from the region of Kozloduy (North Bulgaria) was used in the current experimental study. The index properties of the loess soil were determined according to the BDS EN ISO/TS 17892. Granulometrically, the tested soil is composed of 97% silt and 3% clay fractions. Its density of solid particles is 2.74 g/cm³, and the liquid and plastic limits are 35.6% and 17.3%, respectively. Based on the European Soil Classification System, the loess soil is classified as low plasticity clay (CIL).

As stabilizers, Portland cement and zeolite, both in 10% by the dry weight of soil, were used. The Portland cement was CEM II/B–L 32.5 according to the BDS EN 197–1 classification of cement. This

cement contains 65–79% clinker, 21–35% limestone and up to 5% additional components, and it is recommended for the production of mortar and concrete, as well as for soil stabilization. The used zeolite was obtained from the Beli Plast quarry in the Northeast Rhodopes (Bulgaria). It contains about 70% of clinoptylolite. The grain–size fraction of the zeolite is less than 0.08 mm.

The chemical compositions of the loess, cement and zeolite are presented in the Table 1. The chemical compositions of zeolite and loess soil were identified by using X-ray fluorescence analysis. The loss on ignition (LOI) was determined at 550 °C, because at this ignition temperature 99.8% of the total calcite fraction remains in the soil samples. The chemical composition of the cement was provided by the supplier.

The test specimens were prepared in accordance with JGS 0821–2020 without compaction at 41.5% water content. The molded specimens were sealed and stored in a curing chamber at a relative humidity of 95% and a temperature of 20 °C. After respective curing of 7, 28 and 180 days, the samples were taken out of the molds. After that, small specimens with an approximate volume between 1 cm³ and 1.5 cm³ were cut. Prior to the SEM analyses, the samples were dried with minimum structural disturbance in a vacuum oven at 20 °C. The dried samples were then kept in a desiccator under vacuum until tested.

The SEM analysis was conducted using a JEOL 733 Superprobe SEM and microprobe ORTEC System 5000 equipped with Energy Dispersive Spectroscopy (EDS) (14 kV, 1 nA) at the Geological Institute of the Bulgarian Academy of Sciences. For the SEM analysis, the stabilized loess samples were secured on aluminum mounting stubs by carbon glue and sputters coated with one layer of carbon in order to enhance the conductivity of the tested specimen, and then were coated with a 20-nm layer of gold. The samples were analyzed with a focused electron beam with accelerating voltage of 14 kV and secondary electron images were produced. SEM images were taken at different levels of mag-

Table 1
Chemical composition of the materials used (wt.%)

	SiO ₂	Al ₂ O ₃	Fe ₂ O ₃	CaO	N ₂ O	K ₂ O	MgO	TiO ₂	SO ₃	H ₂ O	LOI
Loess	51.68	11.59	4.12	11.69	0.98	1.49	4.27	0.56	–	1.32	1.32
Zeolite	71.66	10.57	1.09	3.40	0.81	2.82	1.49	0.17	–	5.07	5.07
CEM II	17.82	3.29	2.55	60.78	0.16	0.28	1.61	–	2.52	–	1.40

nification to provide a detailed view of the treated soil matrix. The observations were performed on specimens of untreated loess soil as well. In addition, to identify the formation of new phases, SEM–EDS analyses were carried out.

RESULTS AND DISCUSSION

The SEM micrographs of the undisturbed untreated loess soil taken at different magnifications are presented in Figure 1. The skeleton matrix structure of the intact loess soil is seen at low magnification (Fig. 1a). The aggregates and the inter-aggregate pore spaces are clearly displayed at higher magnification (Fig. 1b). The sizes of particles vary significantly, ranging from 1 μm to 20 μm . These particles are mainly angular to subangular, according to the classification scale developed by Powers (1953), and are randomly distributed and oriented. The placoid and flaky microaggregates were identified as quartz and illite. The inter-aggregate pore space is empty or is filled by calcite and clay cementations, which act as bridging and bonding between particles and provide a relatively high stability of loess structure at unsaturated condition (Liu *et al.*, 2016). Some areas of the sample are dense, while others are very porous.

SEM imaging with EDS was performed on the stabilized loess soil. The SEM micrographs show significant changes in the microstructure of loess soil mixed with Portland cement and zeolite after 7-day curing. The transformation of loess matrix by reaction products and subsequent changes due to hydration reaction are clearly apparent (Fig. 2a). As the studied composite mixture has relatively high water/cement ratio and the soil matrix is porous, the

fibrous growths have the space to develop properly and are clearly distinguishable in the sample. Double *et al.* (1978) reported similar observations. At higher magnification, the rapid initial formation of hydration products was detected (Fig. 2b). The soil particles and the pores are partly covered and filled by fibrous phases with length about 0.5–1.0 μm . Identical fibrous phases were observed in the microstructure of compacted loess–cement after a 7-day curing period by Angelova and Evstatiev (1990).

In order to identify the elemental composition of the developed hydration products, the SEM–EDS spectral analysis was conducted over the marked points (Fig. 2b). Precise analysis of these hydration products in the loess–cement–zeolite by EDS is difficult because of the complex matrix that surrounds them. The results of SEM–EDS analysis are presented in Fig. 2c, d. The spectrum profiles display different charts, depending on the composition and distribution of hydration products developed in the stabilized loess matrix. The semi-quantitative analyses show that, at both selected points, Ca and Si can be detected, which indicates the presence of C–S–H phases. The average Ca/Si ratio in the analyzed points is 1.47 by weight. The high percentage of Ca in the sample after a 7-day curing period confirms the availability of extra compounds for pozzolanic reaction.

Under the SEM, the overall morphology of C–S–H (at normal temperature) can vary from the common fibrous type to irregular grains forming a reticular network (Shondeep *et al.*, 2001). Figure 2b shows fibrous structure of C–S–H.

The generation of C–S–H phases proves that a pozzolanic reaction does take place in the loess soil when cement and zeolite are added. The zeolite addition causes extra changes to the soil matrix due

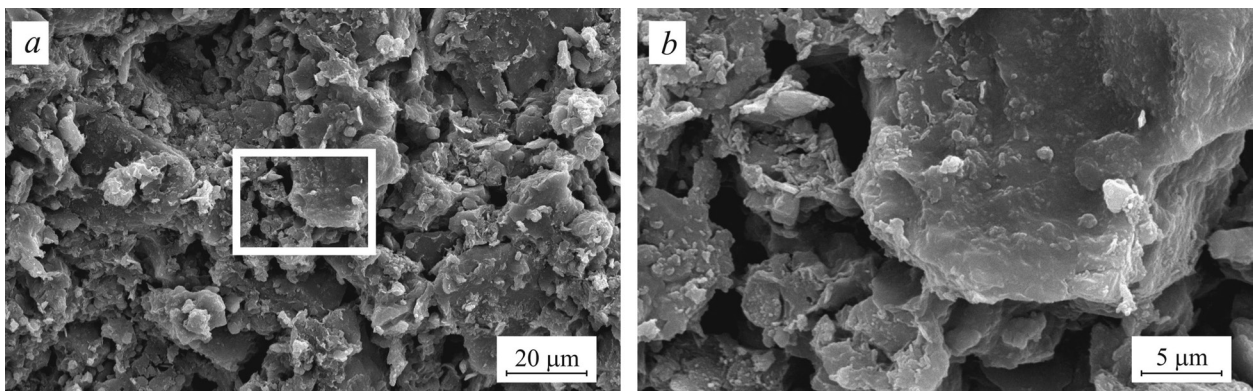


Fig. 1. SEM images of the untreated loess soil: a) $\times 1000$ magnification; b) $\times 4000$ magnification (white rectangle from a).

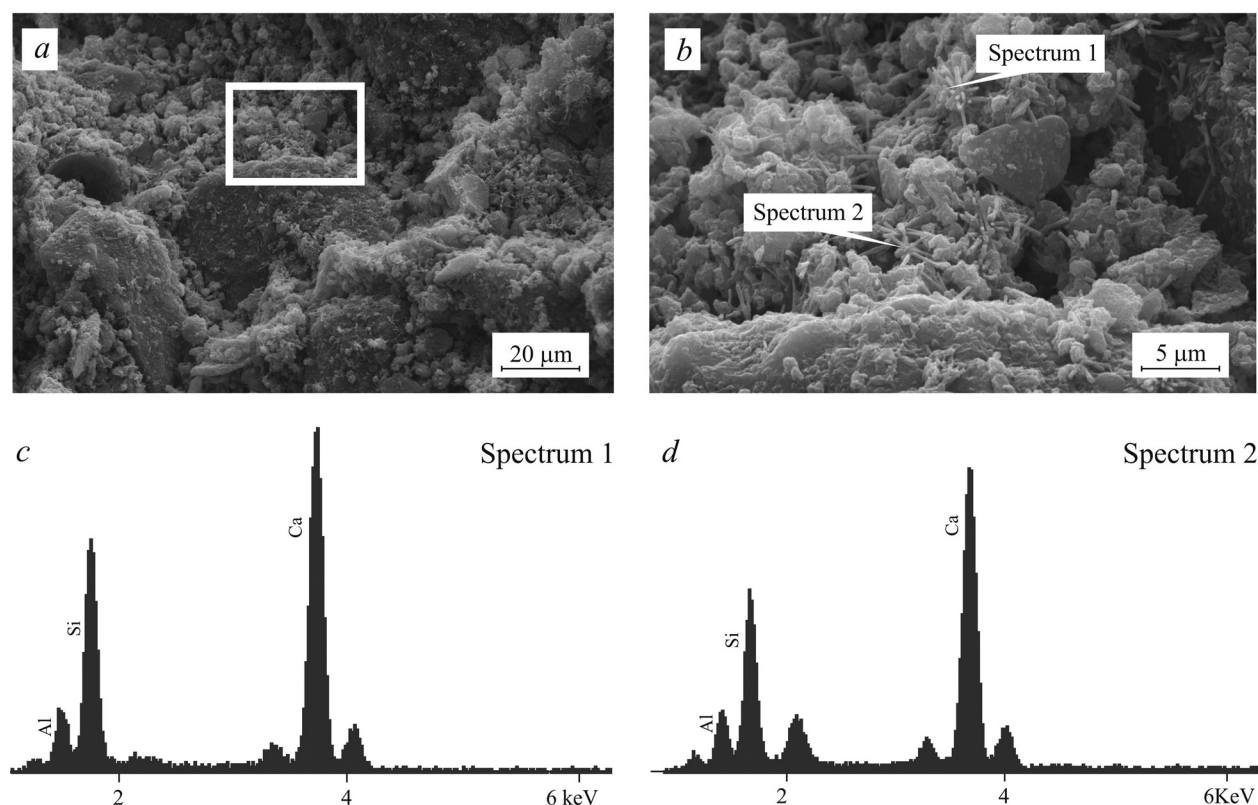


Fig. 2. Stabilized loess soil after 7 days of curing: a) SEM $\times 1000$ magnification; b) SEM $\times 4000$ magnification (white rectangle from a); c) EDS spectrum 1; d) EDS spectrum 2.

to its high cation exchange activity. Snellings *et al.* (2010) reported that the exchangeable cation process, which results in Ca^{2+} ions replacing the Na^+ and K^+ cations from zeolite, also has influence on the pozzolanic activity, distribution and the formation of the reaction products.

As time goes by, the amount of fibrous phases increases. After a 28-day curing period, the hydration products start the formation of a reticular fibrous network (Fig. 3a, b), which was attributed to the C–S–H gel hydration products. The produced C–S–H phases grew remarkably and development of ettringite ($3\text{CaO} \cdot \text{Al}_2\text{O}_3 \cdot 3\text{CaSO}_4 \cdot 32\text{H}_2\text{O}$ or $\text{C}_6\text{AS}_3\text{H}_{32}3\text{CaO}$) was noted. The results from semi-quantitative analyses confirmed that the hydration products consist predominantly of C–S–H phases with $\text{Ca}/\text{Si} = 1.81$ by weight (Fig. 3c), accompanied by smaller amounts of ettringite (Fig. 3d). The EDS spectrum profile in Fig. 3d is characteristic for ettringite, which is one of the primary hydration products. Its formation is a result of the reaction of calcium aluminate (CaAl_2O_4) with calcium sulfate (CaSO_4), both present in Portland cement (Merlini *et al.*, 2008).

When compared with an intact loess SEM micrograph (Fig. 1), the microstructure of treated loess after 28-day curing (Fig. 3a, b) was much denser: the inter-particle spacing has decreased, the bonds between loess particles have increased considerably and the soil–hydration clusters tend to be larger. As reported in previous studies, this leads to strength growth and permeability reduction of the treated soil (Tchakalova and Todorov, 2008; Mola-Abasi *et al.*, 2016; Rajabi and Ardakani, 2020).

The ensuing curing period showed many modifications in the soil microstructure. The soil matrix changes after 180-day curing are illustrated in Fig. 4a, b. At this stage, a greater degree of flocculation than on the 28th day and growth of reaction products were observed. Fibrous and gel-like hydration products were detected and recognized by the SEM–EDS analysis as C–S–H (Fig. 4c, d), with average Ca/Si ratio of 3.04 by weight. The percentages of corresponding chemicals increase with the increase in the curing period up to 180 days. Jha and Sivapullaiah (2015) reported that this increase may be attributed to formation of pozzolanic reaction products.

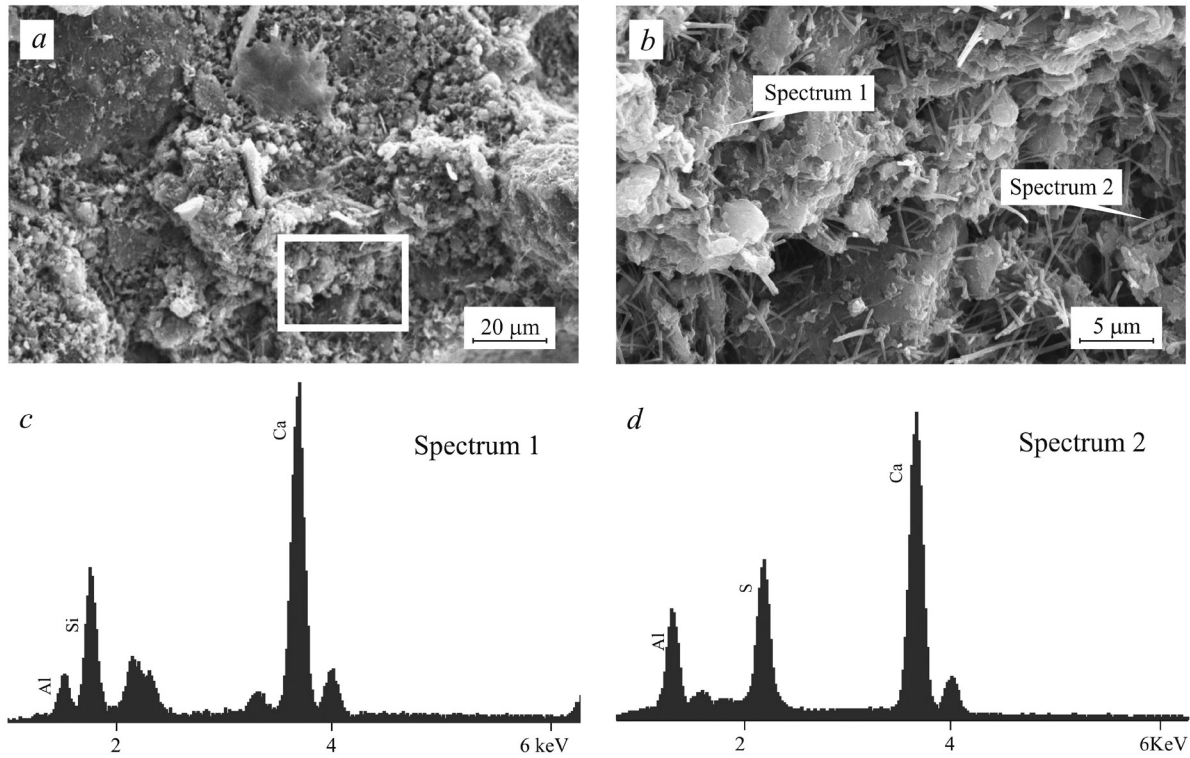


Fig. 3. Stabilized loess soil after 28-day curing: a) SEM $\times 1000$ magnification; b) SEM $\times 4000$ magnification (white rectangle from a); c) EDS spectrum 1; d) EDS spectrum 2.

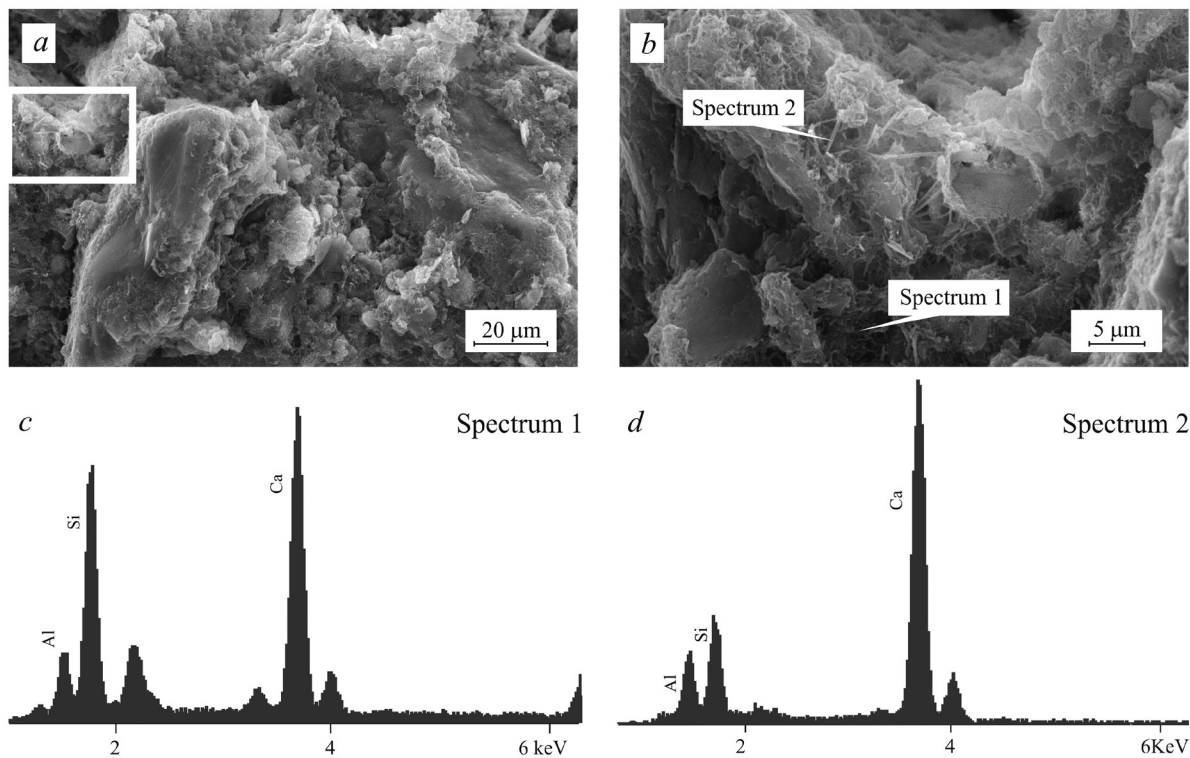


Fig. 4. Stabilized loess soil after 180-day curing: a) SEM $\times 1000$ magnification; b) SEM $\times 4000$ magnification (white rectangle from a); c) EDS spectrum 1; d) EDS spectrum 2.

The preponderance of C–S–H reaction products during all curing time can be linked with the use of medium silica zeolite ($\text{SiO}_2/\text{Al}_2\text{O}_3 = 6.78$, see Table 1) as well. As reported by Liguori *et al.* (2019), the prevalence of Si over Al in the zeolite framework enables fixing a greater amount of Ca at longer curing times, therefore the addition of zeolite raises the pozzolanic activity.

The fibrous phases form bridges between the soil aggregates and the gel-like phases bond aggregates and fill the inter-aggregate pore space. Even though the loess soil is treated without compaction, at higher magnification it is seen that the microstructure of the treated soil matrix is dense (Fig. 4b) and is fully comparable to the improvement with compaction.

CONCLUSIONS

- Based on the study presented in the paper, the following conclusions can be derived:
- Cement–zeolite treatment without compaction of loess soil causes changes in its microstructure;

- SEM images show significant physical modification of the loess soil matrix over time. Micrographs of the treated loess after 180-day curing indicated the presence of dense reticulated compounds among the soil particles, and thereby appearance of compact and non-porous matrix;
- Cementitious materials, such as calcium–silicate hydrate (C–S–H) and ettringite ($3\text{CaO}\cdot\text{Al}_2\text{O}_3\cdot3\text{CaSO}_4\cdot32\text{H}_2\text{O}$ or $\text{C}_6\text{AS}_3\text{H}_{32}3\text{CaO}$), produced over time by cement hydration and pozzolanic reactions, were observed and confirmed by SEM-EDS analysis. C–S–H are the dominant reaction product;
- The Ca/Si ratio in C–S–H phases was found to vary at different curing times between 1.47–3.04, which indicates possible secondary cementitious reactions between the soil and the stabilizers;
- Cement–zeolite treatment without compaction of loess soil can markedly improve its engineering properties, such as collapsibility/compressibility, strength and water-resistance.

REFERENCES

- Angelova, R., Evstatiev, D. 1990. Strength gain stages of soil–cement. *Proceedings of the 6th International IAEG Congress, Amsterdam*, 3147–3154.
- Antonov, D. 2013. Static and dynamic strength parameters of stabilized loess soils from Kozloduy town area. *Engineering Geology and Hydrogeology* 27, 3–12.
- BDS-EN197-1 2011, “BDS-EN197-1. 2011. Cement-Part 1: Composition, specifications and conformity criteria for common cements. Bulgarian Institute for Standardization (in Bulgarian).
- BDS EN ISO/ TS 17892. 2015. *Geotechnical investigation and testing – Laboratory testing of soil, Multi-part Document*. Bulgarian Institute for Standardization (in Bulgarian).
- Double, D., Hellowell, A., Perry, S.J. 1978. The hydration of Portland Cement. *Proceedings of the Royal Society of London. Series A, Mathematical and Physical Sciences* 359 (1699), 435–451, <https://doi.org/10.1098/rspa.1978.0050>.
- Evstatiev, D. 1984. *Strength-Formation of Soil-Cement*. Publishing House of the Bulgarian Academy of Sciences, Sofia, 94 pp. (in Bulgarian).
- Glasser, F., Diamond, S., Roy, D. 1986. Hydration reactions in cement pastes incorporating fly ash and other pozzolanic materials. *MRS Proceedings* 86, 139, <https://doi.org/10.1557/PROC-86-139>.
- JGS 0821-2020 (Japanese Geotechnical Society Standard). 2020. *Practice for Making and Curing Stabilized Soil Specimens without Compaction*, <https://www.jiban.or.jp/e/standards/jgs-standards/>.
- Jha, A.K., Sivapullaiah, P.V. 2015. Mechanism of improvement in the strength and volume change behavior of lime stabilized soil. *Engineering Geology* 198, 53–64, <https://doi.org/10.1016/j.enggeo.2015.08.020>.
- Kamruzzaman, A., Chew, S., Lee, F. 2006. Microstructure of cement-treated Singapore marine clay. *Proceedings of the Institution of Civil Engineers Ground Improvement* 10 (3), 113–123, <https://doi.org/10.1680/grim.2006.10.3.113>.
- Liguori, B., Aprea, P., de Gennaro, B., Iucolano, F., Colella, A., Caputo, D. 2019. Pozzolanic activity of zeolites: the role of Si/Al ratio. *Materials* 12 (24), 4231, <https://doi.org/10.3390/ma12244231>.
- Liu Z., Liu, F., Ma, F., Wang, M., Bai, X., Zheng, Y., Yin, H., Zhang, G. 2016. Collapsibility, composition, and microstructure of loess in China. *Canadian Geotechnical Journal* 53 (4), 673–686, <https://doi.org/10.1139/cgj-2015-0285>.
- Merlini, M., Artioli, G., Cerulli, T., Cella, F., Bravo, A. 2008. Tricalcium aluminate hydration in additivated systems. A crystallographic study by SR-XRPD. *Cement and Concrete Research* 38 (4), 477–486, <https://doi.org/10.1016/j.cemconres.2007.11.011>.
- Mola-Abasi, H., Kordtabar, B., Kordnaeij, A. 2016. Effect of natural zeolite and cement additive on the strength of sand. *Geotechnical and Geological Engineering* 34 (5), 1539–1551. <https://doi.org/10.1007/s10706-016-0060-4>.
- Nontananandh, S., Yoobanpot, T., Boonyong, S. 2005. Scanning electron microscopic investigations of cement stabilised soil. *National Conference on Civil Engineering No. 10, Thailand, GTE*, 23–26.

- Poon, C.S., Lam, L., Kou, S.C., Lin, Z.S. 1999. A study on the hydration rate of natural zeolite blended cement pastes. *Construction and Building Materials* 13 (8), 427–432, [https://doi.org/10.1016/S0950-0618\(99\)00048-3](https://doi.org/10.1016/S0950-0618(99)00048-3).
- Powers, M.C. 1953. A new roundness scale for the sedimentary particles, *Journal of Sedimentary Petrology* 23, 117–119, <https://doi.org/10.1306/D4269567-2B26-11D7-8648000102C1865D>.
- Quadri, H.A., Abiola, O.S., Odunfa, S.O., Azeez, J.O. 2022. Evaluation of strength and microstructural characteristics of weak lateritic soil stabilized with calcined clay and iron slag dust. In: Tutumluer, E., Nazarian, S., Al-Qadi, I., Qamhia, I.I. (Eds), *Advances in Transportation Geotechnics IV. Lecture Notes in Civil Engineering* 164, 781–793, https://doi.org/10.1007/978-3-030-77230-7_59.
- Rajabi, A.M., Ardakani, S.B. 2020. Effects of natural-zeolite additive on mechanical and physicochemical properties of clayey soils. *Journal of Materials in Civil Engineering* 32 (10), 4020306, [https://doi.org/10.1061/\(ASCE\)MT.1943-5533.0003336](https://doi.org/10.1061/(ASCE)MT.1943-5533.0003336).
- Romero, E. 2013. A microstructural insight into compacted clayey soils and their hydraulic properties. *Engineering Geology* 165, 3–19, <https://doi.org/10.1016/j.enggeo.2013.05.024>.
- Salamatpoor, S., Jafarian, Y., Hajannia, A. 2018. Improving shallow foundations resting on saturated loose sand by zeolite-cement mixture: A laboratory study. *Scientia Iranica* 25 (4), 2063–2076, <https://doi.org/10.24200/SCI.2018.50153.1567>.
- Shondeep, L.S., Xu, A., Dipayan, J. 2001. Scanning electron microscopy, X-ray microanalysis of concretes. In: Ramachandran, V.S., Beaudoin, J.J. (Eds), *Handbook of Analytical Techniques in Concrete Science and Technology*. Noyes Publications, New Jersey and William Andrew Publishing LLC, New York, 231–274, <https://doi.org/10.1016/B978-081551437-4.50010-2>.
- Snellings, R., Mertens, G., Cizerb, Ö., Elsen, J. 2010. Early age hydration and pozzolanic reaction in natural zeolite blended cements: Reaction kinetics and products by in situ synchrotron X-ray powder diffraction. *Cement and Concrete Research* 40 (12), 1704–1713, <https://doi.org/10.1016/j.cemconres.2010.08.012>.
- Tchakalova, B., Todorov, K. 2008. Plastic soil cement mixtures for isolation barriers. *Geologica Balcanica* 37 (1–2), 91–96.
- Türköz, M., Vural, P. 2013. The effects of cement and natural zeolite additives on problematic clay soils. *Science and Engineering of Composite Materials* 20 (4), 395–405, <https://doi.org/10.1515/secm-2012-0104>.
- Ural, N. 2021. The significance of scanning electron microscopy (SEM) analysis on the microstructure of improved clay: An overview. *Open Geosciences* 13 (1), 197–218, <https://doi.org/10.1515/geo-2020-0145>.